

1       **Comparative assessment of adsorbents performances of plant**  
2       **biomasses grown on different sites: case study of invasive**  
3       ***Acer negundo* L.**

4       TATJANA ŠOŠTARIĆ<sup>1\*</sup>, ZORICA LOPIČIĆ<sup>1</sup>, DRAGANA RANĐELOVIĆ<sup>1</sup>, TAMARA  
5       RAKIĆ<sup>2</sup>, ANJA ANTANASKOVIĆ<sup>1</sup>, IVANA MIKAVICA<sup>1</sup> and SNEŽANA ZILDŽOVIĆ<sup>1</sup>

6       <sup>1</sup>*Institute for Technology of Nuclear and Other Mineral Raw Materials, Boulevard Franchet*  
7       *d'Esperrey 86, 11000 Belgrade, Serbia and* <sup>2</sup>*University of Belgrade, Faculty of Biology,*  
8       *Studentski trg 16, 11000 Belgrade, Serbia*

9       (Received 8 May, revised 11 June, accepted 12 August 2025)

10       *Abstract:* With the increasing global spread of invasive species, collecting  
11       their biomass could be a promising source for adsorbent development and water  
12       remediation. Therefore, the ability of adsorbent based on biomass of invasive plant  
13       *Acer negundo* L. originating from different habitat types was investigated for the  
14       lead removal from aqueous solution, in order to observe if different growing sites  
15       have effect on adsorbent performances. Three sites were selected for sampling:  
16       forest edges on Mt. Avala, riparian forests at Great War Island and banks of coal  
17       separation pond in Piskanja. Characterisation was performed *via* pH<sub>pzc</sub>, zeta  
18       potential, CEC, SEM-EDS and FTIR analysis. Optimization of sorption parameters  
19       was done and the best performance was at pH 5.0, adsorbent dosage 2.0 g/dm<sup>3</sup> at  
20       298 K for 60 min. Fitting of isothermal experiment data showed best correlation  
21       with Sips model ( $q_{\max}$  is 94.92–131.52 mg/g, according to growing site). Among  
22       three reaction kinetic models, pseudo-second-order kinetics model showed best  
23       results. Since sample taken from the most anthropogenic influenced area have  
24       almost 30% lower adsorption capacity than others, it can be concluded that  
25       growing site characteristics reflect on biomass performances, which is important  
26       factor for any further biomass usage.

27       *Keywords:* adsorption; invasive plants; *Acer negundo* L.; lead; kinetics.

28       INTRODUCTION

29       *Acer negundo* L. which originates from North America, was introduced to  
30       Europe as a cultivated woody species in the 17<sup>th</sup> century and was planted in the  
31       cities due to its rapid growth and resistance to weather extremes. It is still one of

---

\* Corresponding author. E-mail: t.sostaric@itnms.ac.rs  
<https://doi.org/10.2298/JSC250508065S>

32 the most common species in parks, street tree lines, and spontaneously occurs  
33 along roads and in other disturbed habitats. However, it has become invasive in  
34 both natural and urban habitats.<sup>1</sup> *A. negundo* has broad ecological amplitude: it  
35 tolerates air pollution, soils with wide range of pH values, extreme cold and  
36 drought.<sup>2</sup> In Serbia, *A. negundo* is considered as one of the most aggressive  
37 invasive tree species in forest ecosystems and its presence has also been detected  
38 in many areas with preserved natural values.<sup>3</sup>

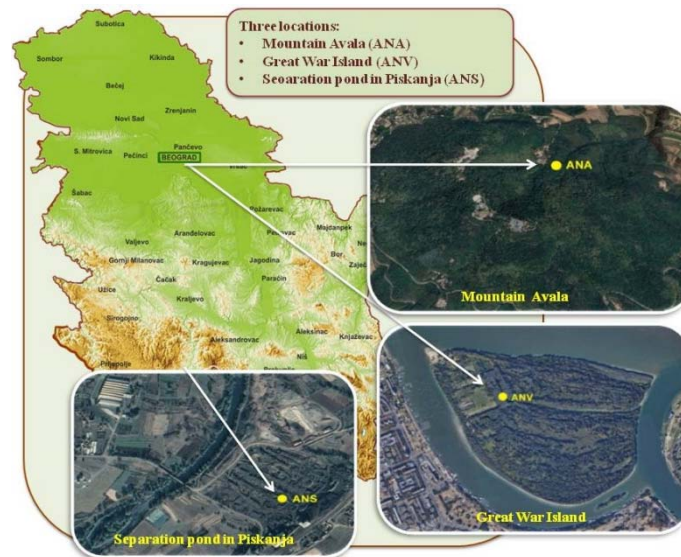
39 Abundant biomass of invasive plant species is nowadays recognized for its  
40 potential benefits in providing various environmental services. Adsorption, as one  
41 of the sustainable and efficient remediation technique could be potential field for  
42 its application. Moreover, adsorption is considered as a cost-effective and reliable  
43 method for purification of contaminated water, especially in the case of common  
44 water metal pollutants.<sup>4</sup> Plant-derived materials such as wood, leaves, fruits, or  
45 seeds have been studied for this purpose, where adsorbents based on leaf biomass  
46 showed the best adsorption performance.<sup>5</sup> Biomass of *Acer* species have been  
47 tested as adsorbents for metal removal from aqueous solutions,<sup>6</sup> but no such  
48 studies have been conducted on invasive *A. negundo*. Also, so far there has been  
49 lack of investigations concerning sorption performance of biomasses of the same  
50 species collected from different habitats. Therefore, the research questions aimed  
51 to answer were: *a*) is invasive *A. negundo* leaf biomass suitable adsorbent for metal  
52 aqueous pollution? *b*) does the *A. negundo* leaves originated from sites with  
53 contrasting ecological, edaphic and anthropogenic differ in their composition and  
54 *c*) does the leaf composition variability impact metal adsorption capacity?

## 55 EXPERIMENTAL

56 Three different growing sites were selected for sampling *A. negundo* leaves. First sampling  
57 site, Mt. Avala, represents protected area in the vicinity of Belgrade, with environment that  
58 supports a large diversity of species. It is recognized as Emerald Network site and as a Serbian  
59 ecological network site.<sup>7</sup> Seven allochthonous invasive tree species were recorded on Mt.  
60 Avala, including *A. negundo*.<sup>8</sup> Area of the natural landscape Great War Island, the second  
61 sampling site, represents unique example of protected area located in the urban environment of  
62 Belgrade. The island is habitat for many species and it is being annually flooded by the Danube  
63 River. It is recognized as one of the central areas of Serbia's ecological network and the  
64 ecological Network within the Danube ecological corridor.<sup>9,10</sup> However, research of Kašanin *et*  
65 *al.*<sup>11</sup> showed increased pollution of Great War Island sediments with Cu and Cd, as well as with  
66 oil pollutants. In the area of Great War Island 17 invasive tree species, among which is *A.*  
67 *negundo*, are registered.<sup>12</sup> Third sampling point is placed on the banks of former coal separation  
68 pond in Piskanja, which is a part of industrial setting at Ibar coal mining basin in South-Central  
69 Serbia. This area is nowadays sporadically colonized by various plant species, including  
70 invasive ones.<sup>13</sup> Sampling points are presented in Fig. 1.

71 Composite soil samples were taken at each sampling site from the upper layer (0–20 cm)  
72 of the rhizosphere zone. Soils were air-dried and sieved through 2 mm sieve. Pseudo-total  
73 content of elements was determined by using aqua region digestion following ISO 11466:1995

74 standard<sup>14</sup> and measured by AAS. The content of soil organic carbon (SOC) was determined by  
 75 oxidation with a solution of  $\text{KMnO}_4$  according to the Koltzman method.<sup>15</sup>



76  
 77 Fig. 1. Sample points: forest edges on Mt. Avala (a), riparian forests at Great War Island (b)  
 78 and banks of former coal separation pond in Piskanja (c).

79 Up to 100 fully developed leaves from mature *A. negundo* trees were collected during June  
 80 from middle canopy section and each side of the crown of 3–5 individuals of approximately  
 81 similar age, in order to make representative composite samples for each sampling site. Leaves  
 82 were collected by pruning following methodology described elsewhere<sup>16</sup>. They were rinsed  
 83 with distilled water and air-dried. Leaves were then grinded in blade grinder (20.000–30.000  
 84 rpm) and powdered prior to analysis (particle size < 0.2 mm). Samples from Mt. Avala, Great  
 85 War Island and coal separation pond Piskanja were labelled as ANA, ANV and ANS, respective-  
 86 tively, as presented in Fig. 1. In order to determine the content of elements, the samples were  
 87 dissolved using standardized microwave-assisted acid dissolution procedure for this type of  
 88 material in High-performance Microwave Digestion System ETHOS UP, Milestone and the  
 89 concentrations of elements were determined by atomic absorption spectrometry (AAS), while  
 90 K, Ca and Na were determined by atomic emission spectrometry using PerkinElmer PinAAcle  
 91 900T, USA, directly from the prepared solution. Bioconcentration factor (BCF) was used to  
 92 determine the efficiency of metal accumulation in leaves, and it was calculated as a ratio  
 93 between metal concentration in leaves and pseudo-total concentration of the same element in  
 94 the soil.<sup>17</sup> Cation exchange capacity (CEC) was determined by method that involves saturation  
 95 of the cation exchange sites by ammonium acetate.<sup>18</sup> Determination of pH value of suspensions  
 96 ( $\text{pH}_{\text{sus}}$ ) was performed according to standard ASTM D6851-02. Determination of the point of  
 97 zero charge ( $\text{pH}_{\text{pzc}}$ ) was done in accordance to methodology described elsewhere.<sup>19</sup> In order to  
 98 determine zeta potential of samples Zetasizer Nano Z (Malvern, U.K.) was used in the pH range  
 99 from 2.0 to 10. In order to observe surface morphology and elemental composition of leaf  
 100 powder, scanning electron microscopy combined with the energy dispersive spectroscopy  
 101 (JEOL JSM 6460, JEOL Ltd., Japan) was used. The dried samples were coated with thin layer

102 of gold under vacuum conditions. Attenuated Total Fourier Transform Infrared Spectroscopy  
 103 was used for determination of samples surface functional groups by using Thermo Nicolet 6700  
 104 FTIR (Thermo Fisher Scientific, United States). The spectra were recorded in range from 4000  
 105 to 400  $\text{cm}^{-1}$ . The region between 1900 and 2200  $\text{cm}^{-1}$  is interrupted due to strong diamond IR  
 106 absorption.

107 Batch sorption experiments were performed through the sets of the experiments where one  
 108 parameter was varied, while the others remained constant. Experiments were performed by  
 109 mixing sample with metal solution and stirring it on orbital thermostatic shaker (Heidolph-  
 110 Unimax 1010, USA) at 200 rpm. Lead stock solution (1.0 mmol/dm<sup>3</sup>) was prepared from  
 111 Pb(NO<sub>3</sub>)<sub>2</sub>·3H<sub>2</sub>O (analytical grade). After investigated period of time suspension was filtrated  
 112 and the filtrate was analysed using AAS. The effects of following parameters on sorption capaci-  
 113 ty were analysed: a) Effect of initial pH in the range from 2.0 to 5.0; b) Effect of contact time  
 114 in range from 2 to 180 min; c) Effect of sorbent concentration in range from 1 to 20 g/dm<sup>3</sup>; d)  
 115 Effect of initial lead concentration in range from 5 to 600 mg/dm<sup>3</sup>; e) Effect of temperature in  
 116 range from 288 to 328 K. The sorption capacity was calculated using the following equation:

$$117 \quad q_e = \frac{(C_o - C_e)V}{m} \quad (1)$$

118 Where  $q_e$  is the amount of lead absorbed (mg/g);  $C_o$  and  $C_e$  are the initial and equilibrium  
 119 lead concentrations (mg/dm<sup>3</sup>);  $V$  - the sorbate solution volume (dm<sup>3</sup>);  $m$  - the sorbent mass (g).  
 120 The involvement of ion-exchange mechanism during the sorption process was investigated by  
 121 following the release of cations (Ca<sup>2+</sup>, Mg<sup>2+</sup>, Na<sup>+</sup>, K<sup>+</sup> and H<sup>+</sup>) from sorbents after process of  
 122 lead sorption. The ratio was calculated by using the following equation:

$$123 \quad R_{b/r} = \frac{[\text{Pb}^{2+}]}{[\text{Ca}^{2+}] + [\text{Mg}^{2+}] + \frac{[\text{Na}^+]}{2} + \frac{[\text{K}^+]}{2} + \frac{[\text{H}^+]}{2}} \quad (2)$$

124 where  $R_{b/r}$  is the ratio of the bonded lead ions and released cations, while in brackets are  
 125 amount of bonded lead ions and amounts of specific cations released from sorbents.

126 Kinetic and isotherm investigations were performed in order to analyse the sorption  
 127 process, fitting the experimental sorption data by various isotherm and kinetic models, which  
 128 might elucidate the nature of sorption process. Kinetic and isothermal experimental data were  
 129 obtained from the experiments performed under optimised operational parameters ( $C_{\text{Pb}^{2+}}=200$   
 130 mg/dm<sup>3</sup>,  $m/V=2.0$  g/dm<sup>3</sup>,  $pH=5.0$ ,  $T=298$  K, and  $t=180$  min). Isothermal sorption experiments  
 131 were conducted under the same operational parameters, varying initial lead concentration from  
 132 5.0 up to 600 mg/dm<sup>3</sup>. Models/equations which have been used in this paper are presented in  
 133 Table S1. All sorption experiments were performed in triplicate and results were reported as  
 134 arithmetic mean values. The statistical analysis was performed and nonlinear correlation coef-  
 135 ficient ( $R^2$ ) and the reduced chi square test ( $\chi^2$ ) were applied to measure the appropriateness of  
 136 applied kinetic and isotherm models.

137 Soil and plant analysis were carried out in triplicates, and the results are presented as  
 138 arithmetic means  $\pm$  standard deviations. Statistical differences between sites and concentration  
 139 of elements in plant leaves were determined by using one-way analysis of variance (ANOVA)  
 140 in Statistica 8.0 (StatSoft 2007).

141

## RESULTS AND DISCUSSION

142 *Characterization of samples*

143 Invasive plant species exhibit broad ecological amplitude that allows them to  
144 colonize ecologically diverse habitats. Due to developmental plasticity, the same  
145 plant species grown on ecologically different habitats might show significant  
146 variation in structural and physiological traits.<sup>20</sup> Plant leaves are considered to be  
147 among most sensitive organs to the influence of environmental factors, showing  
148 differences in chemical components and presence of functional groups.<sup>21</sup> In  
149 relation to that, characterization of collected samples of soil and leaf biomass was  
150 conducted. The measurements of the soil pH, content of soil organic carbon (SOC),  
151 concentration of potentially toxic elements (PTE) and macroelements in topsoil  
152 layers (0–20 cm), together with concentrations of PTE in leaves are presented in  
153 TABLE S2 (Supplementary material). Soil pH ranges from neutral (ANA<sub>S</sub>) and  
154 slightly acid (ANV<sub>S</sub>), to acidic (ANS<sub>S</sub>), while content of SOC shows higher values  
155 on ANA<sub>S</sub>. On this site, value of Pb content is high, which is in line with results of  
156 Stanković *et al.*<sup>22</sup> for the same site. Highest concentration of Fe and Ni due to the  
157 present technogenic pollution is recorded for soils of separation pond (ANS<sub>S</sub>),  
158 which is in accordance with investigation of Randelović *et al.*<sup>13</sup>. Content of  
159 macroelements varies significantly between the sites, whereas all of them, except  
160 Na, show the lowest concentration at ANS<sub>S</sub>. The content of measured elements in  
161 plant leaves remains in the range of normal<sup>23</sup> except in the case of Ni that shows  
162 excess values for all sites. As expected, the highest concentration of Ni and Cd are  
163 recorded on *A. negundo* leaves from coal separation pond (ANS<sub>L</sub>). Content of Ca  
164 and Mg significantly differs in leaves originating from different sites, showing the  
165 lowest concentration in ANS<sub>L</sub>, while concentration of K exhibited highest values  
166 on the same site. Similarly, Liu *et al.*,<sup>24</sup> compared leaf mineral content in healthy  
167 and declining *Acer saccharum* stand and find out significantly lower concentration  
168 of leaf Ca and Mg in declining stand in comparison to healthy, and higher  
169 concentration of leaf K in declining in comparison to healthy stand. Role of K is  
170 recognized in the synthesis of protein and carbohydrate metabolism for alleviation  
171 of increased abiotic stresses<sup>25</sup> and Drzewiecka *et al.*<sup>26</sup> have found that K was  
172 mainly transported and accumulated in the aerial organs of *Acer platanoides*  
173 cultivated on polluted mine sludge, accompanied by ROS scavenging and  
174 accumulation of secondary metabolites in plant leaves.

175 Metal uptake from the soil by plant, expressed as BCF factor is presented in  
176 TABLE S3. A value of BCF below 1 refers to the low accumulation of element in  
177 plant organs which is the case for all investigated elements, except Mn, on sites  
178 ANA and ANV.

179 In order to determine capability of leaf samples (future adsorbents) to  
180 exchange cations under chemically neutral conditions, CEC was detected. It is

181 evident from TABLE I that ANS, originating from most anthropogenically  
 182 influenced area, has the lowest total CEC despite the fact that it has 40% and 15%  
 183 higher amount of K ions in comparison to ANA and ANV, respectively.

184 TABLE I. The values of CEC,  $\text{pH}_{\text{pzc}}$ ,  $\text{pH}_{\text{sus}}$  for ANA, ANV and ANS

	K (meq/100g)	Na (meq/100g)	Ca (meq/100g)	Mg (meq/100g)	Total $\Sigma$	$\text{pH}_{\text{pzc}}$	$\text{pH}_{\text{pzc}}$
ANA	36.57	7.35	52.40	73.84	170.16	4.14	3.95
ANV	45.91	7.44	49.90	62.11	165.36	4.12	4.07
ANS	52.62	7.33	37.43	47.72	145.09	4.08	3.72

185 According to Kashyap *et al.*<sup>28</sup> excess K may induce deficiency of other  
 186 nutrients like Mg and Ca, which is in accordance with results from TABLE S2  
 187 (amount of Ca and Mg is noticeably lower in ANS). Lower value of Ca and Mg  
 188 content in leaves, was noted by Liu *et al.*,<sup>24</sup> in declining *Acer saccharum* stands  
 189 developing on acidic soil, too. It is recognized that Ca and Mg deficiencies are  
 190 commonly distributed on acid soils, as such environment promotes leaching of  
 191 these cations<sup>29</sup> which is in accordance with obtained result of ANS soil pH value  
 192 (4.76). The results of point of zero charge ( $\text{pH}_{\text{pzc}}$ ) were explained elsewhere.<sup>30</sup>  
 193 The results of zeta potential values (Fig. S-1.) indicate that in all samples the  
 194 negatively charged surface functional groups are predominant.

195 In order to observe and analyse surface morphology and chemical composition  
 196 of investigated samples, SEM micrographs and corresponding EDS spectra of  
 197 samples are presented in Fig. 2. Heterogeneous structures of samples (cracks,  
 198 irregular pores and rough surface with parts of tracheid) have been described  
 199 elsewhere.<sup>31</sup> Such morphology promotes metal ions diffusion into internal layers  
 200 where numerous active sites become more available for ions, and thus increase  
 201 adsorption performances of sorbent.

202 ATR-FTIR characterization (Fig.S-2.) was carried out, in order to understand  
 203 changes that occurred in surface functional groups from populations from different  
 204 habitats. Despite ATR-FTIR spectra of ANV and ANA samples appear to be very  
 205 similar, certain differences in spectra of ANS sample can be noticed: i) higher  
 206 relative intensity of  $1731\text{ cm}^{-1}$  bend (that refers to the C=O stretching vibration of  
 207 esters from lipid and protein components of cell walls, according to Deng *et al.*<sup>32</sup>),  
 208 ii) the appearance of the shoulder on  $1645\text{ cm}^{-1}$  (also C = O stretching of amide I  
 209 proteins, according to Azuma *et al.*<sup>33</sup>), iii) absence of  $1548\text{ cm}^{-1}$  peak related to  
 210 N-H or C-N stretching of amide II<sup>34</sup>), iv) presence of  $1516\text{ cm}^{-1}$  peak related C=C  
 211 stretching of proteins (amide II), v) lower intensity of the band  $1317\text{ cm}^{-1}$  related  
 212 to the C-H of the methyl functional groups and vi) appearance of the new band at  
 213  $1205\text{ cm}^{-1}$ , due to C-O bending vibration of carbohydrate functional groups.<sup>32</sup>  
 214 This result points out to the involvement of different mechanisms of leaves in  
 215 coping with metal stress common to various plant species, such as impact on

216 protein synthesis and their modification, as well as change in carbohydrate  
 217 metabolism and signalling to oxidative stress regulation.<sup>35</sup>

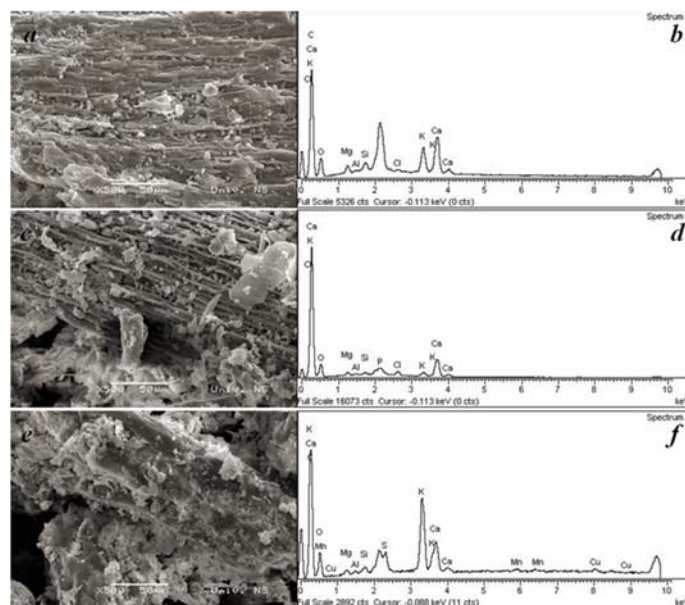


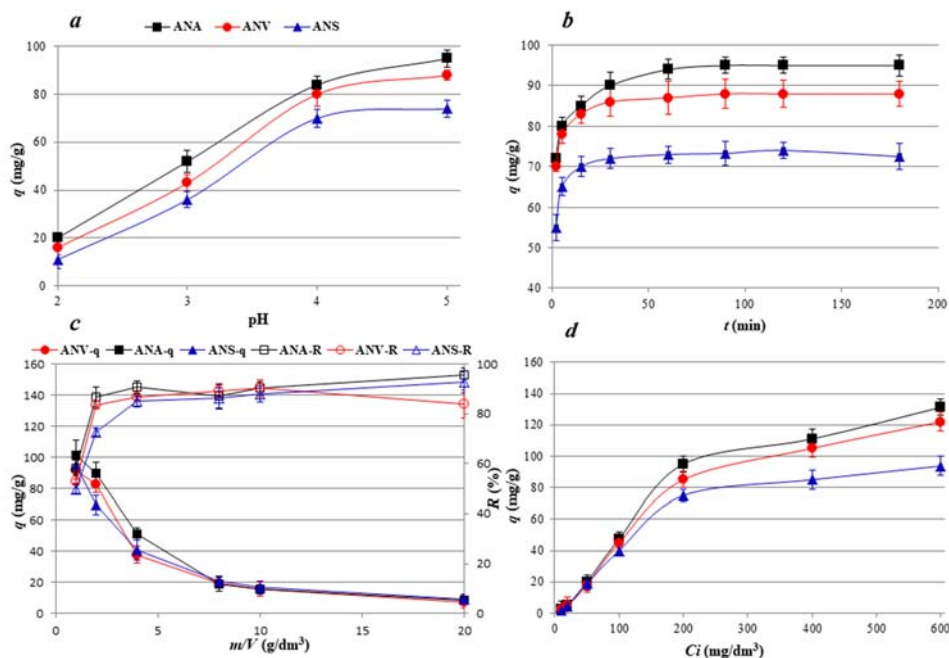
Fig.2. SEM micrographs and EDS spectrums of: ANA (a/b), ANV (c/d) and ANS (e/f).

218  
 219

220 *Sorption studies*

221 Investigation of the effect of pH onto sorption capacity (Fig. 3a) showed the  
 222 same trend for all three samples: low sorption capacity of sorbents at pH 2.0, which  
 223 slowly rises with increase of pH value of the solution. It is well known that solution  
 224 pH affects the dissociation of functional groups present on the sorbent surface: as  
 225 the pH value increases, de-protonation of functional groups occurs and the  
 226 negative charge density increases, increasing the removal of cations from the  
 227 solution. Since the sorption process is the most efficient at pH 5.0 and in order to  
 228 avoid formation of hydroxides which may occur at higher pH values, all further  
 229 experiments were carried out at that pH value. The effect of contact time was  
 230 examined in order to define required time for equilibrium to be reached. As can be  
 231 seen from Fig. 3b, the initial sorption of  $Pb^{2+}$  occurs very rapidly due to available  
 232 and abundant active sites present on sorbents surface, sorption of lead ions  
 233 increases over time and reaches equilibrium after 60 min. The effect of sorbent  
 234 concentration on sorption capacity and removal percentage was also investigated  
 235 and results are presented in Fig. 3c. At sorbent concentration of 1.0 g/dm<sup>3</sup>, lead  
 236 removal percentage was 58, 53 and 49% for ANA, ANV and ANS, respectively.  
 237 However, when sorbent concentration was raised to 2.0 g/dm<sup>3</sup> the percentage of  
 238 lead removal increased up to 87, 84 and 73%, respectively. With further increase

239 of sorbent concentration (up to 20 g/dm<sup>3</sup>), the percentage of lead removal went up  
 240 to 93, 93 and 84%, while the sorption uptake decreased drastically (from 90, 87  
 241 and 70 mg/g to 8.3, 7.5 and 8.9 mg/g, respectively). In relation to that, sorbent  
 242 concentration of 2.0 g/dm<sup>3</sup> was used in all further experiments. Rise of sorbent  
 243 concentration induces particle aggregation and stirring difficulties, consequently  
 244 reducing effective surface area and number of available active sites and slowing  
 245 down the mass transfer.<sup>16</sup> The results of effect of initial lead concentration on  
 246 sorption capacity are presented in Figure 3d. Noticeably, the sorption capacity  
 247 increased, at initial concentration 2.0 mg/dm<sup>3</sup>, from 2.3, 2.4 and 1.8 mg/g to 90.5,  
 248 86.25 and 73.75 mg/g at initial concentration 200 mg/dm<sup>3</sup>, for ANA, ANV and  
 249 ANS, respectively. It is well known that increase of initial metal concentration is  
 250 a driving force for overcoming mass transfer resistance of cations in solid/liquid  
 251 phase.<sup>16</sup> Effect of temperature on lead sorption capacity of tested sorbents was  
 252 investigated and the obtained results are presented at Fig. S-3. As the temperature  
 253 increases, the biosorption capacity decreases from 89.5, 87.7 and 75.7 mg/g at 288  
 254 K to 84.1, 81.7 and 69.25 mg/g at 328 K for ANA, ANV and ANS, respectively.  
 255 Sorption process of lead ions onto investigated sorbents is an exothermic process:  
 256 an increase in temperature lead to decrease in ions removal and temperature rise  
 257 weakens attractive forces between active sites on the sorbent surface and lead ions  
 258 in solution.



259  
 260  
 261

Fig. 3. Effect of operative parameters onto sorbent capacity: effect of pH (a), contact time (b), sorbent concentration (c) and initial  $Pb^{2+}$  concentration (d)

262 *Investigation of ion exchange mechanism*

263 Since analyses of the CEC showed that all samples have cations in exchan-  
264 geable positions, the participation of the ion-exchange mechanism in sorption  
265 process is expected. Consequently, releases of the exchangeable cations from all  
266 materials, together with solution pH value before and after the sorption process,  
267 were investigated and the data are presented in the TABLE S4. Fig. 4 revealed that  
268 the sum of cations, released from ANA and ANV samples, was almost equal to the  
269 amount of  $Pb^{2+}$  bound on the same sorbents, except at lowest metal concentration,  
270 suggesting that ion-exchange mechanism is dominant during the lead sorption  
271 process in both samples. However, the sum of the released cations from sorbent  
272 ANS is higher than concentration of bonded lead ions. ANS bonds reduce lead ions  
273 which are in correlation with lower amount of exchangeable cations on its surface  
274 (TABLE I). These results are in accordance with TABLE S4. Also, the measured  
275 final pH value of the solution after sorption process was 3.77 (lower than initial  
276 pH value - pH 5.0) indicating that ANS releases a significant amount of competitive  
277 hydrogen (hydronium) ions, which reduces binding of lead. This phenomenon  
278 might reflect differences in composition of functional groups and active binding  
279 sites of sorbents originating from different growing sites, as supported by FTIR  
280 analysis.

281 *Kinetic, sorption isotherm and thermodynamic studies*

282 TABLE II summarizes data for experimental sorption capacity at maximum  
283 time investigated ( $q_e$ ), together with the kinetic and isotherm model parameters  
284 and corresponding determination coefficients ( $R^2$ ) and  $\chi^2$  values. The results of  
285 fitting experimental data showed that the best fit was obtained by using the pseudo  
286 second order kinetic model, with the highest values of correlation coefficient ( $R^2$ )  
287 and the lowest chi-factor ( $\chi^2$ ) among the all models applied. This indicates that the  
288 sorption mechanism is limited by bonding forces through sharing electrons  
289 between the sorbate and the sorbents. As can be seen from TABLE II, Lagergren  
290 pseudo-first order equation, as well as Elovich model, cannot be used to predict  
291 the sorption kinetic of lead by any sorbent investigated; the application of this  
292 models resulted in the lower values of  $R^2$  and the higher  $\chi^2$  values, but also  
293 calculated  $q_m$  values differ from experimental  $q_e$  values. The graphs of kinetics  
294 models are presented in Figs. S-4 to S-6.

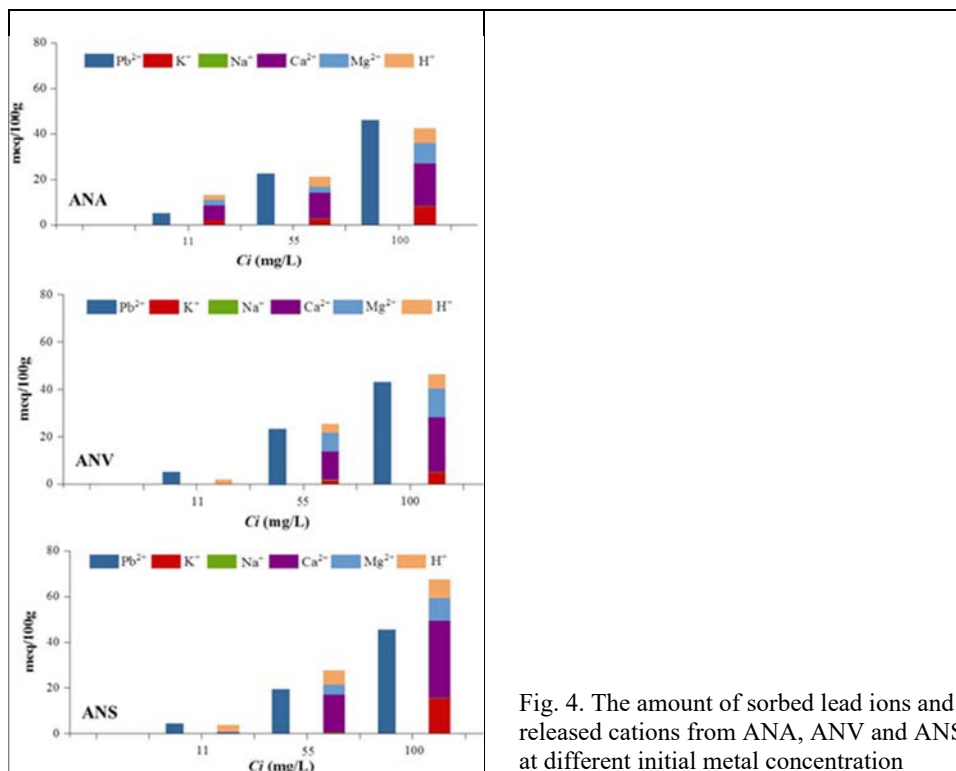


Fig. 4. The amount of sorbed lead ions and released cations from ANA, ANV and ANS at different initial metal concentration

295 The applicability of pseudo-second order kinetics model suggested that the  
 296 lead removal by *A. negundo* sorbents is based on chemical reaction, involving the  
 297 exchange of electrons between the sorbents and the metal ions present in sorbate  
 298 solution. The highest value of the pseudo-second reaction rate constant,  $k_2$ , is  
 299 obtained for ANV sorbent (0.0830 g / (mg min), indicating the fastest removal for  
 300 this sorbent. This can also be seen from the Figure S-4, where the fitting of the  
 301 experimental data by pseudo-second order model is presented. Although the  
 302 highest rate is observed for ANV, the ANA sorbent has higher overall maximum  
 303 sorption capacity under applied operational parameters, 86.04 mg/g, while the  
 304 lowest one is found to be the capacity of ANS (73.67 mg/g). Previous reports on  
 305 sorption kinetics by the similar biomasses suggest that pseudo-second order  
 306 kinetics govern most of the sorption processes. For example, Qaiser *et al.*<sup>36</sup> have  
 307 investigated the potential of *Ficus religiosa* leaves in lead sorption, and find out  
 308 that the sorption process is well described by the pseudo-second order model, with  
 309 maximum removal capacity of 19.76 mg/g at 20°C. Sangi *et al.*<sup>37</sup> have investigated  
 310 the potentials of *Ulmus* sp. and *Fraxinus* sp. tree leaves for lead removal and  
 311 obtained the kinetic results which indicated that second-order kinetics best  
 312 describe the experimental data, relying on the assumption that the rate limiting step

313 involves valence forces through sharing or exchange of electrons between the  
 314 sorbent surface sorbent and sorbate ions. Additional, two-parameter model were  
 315 used to correlate isotherm data: the Langmuir<sup>38</sup> equation which is valid for  
 316 monolayer sorption onto a surface with a finite number of identical sites and the  
 317 empirical Freundlich<sup>39</sup> isotherm based on sorption on a heterogeneous surface.  
 318 Beside them one three-parameter model, named Sips<sup>40</sup> isotherm was used. This  
 319 model represents combination of Langmuir and Freundlich expressions: at low  
 320 metal concentration it approaches Freundlich isotherm, while at high  
 321 concentrations it predicts a monolayer adsorption capacity characteristic for the  
 322 Langmuir isotherm. Graph of all isotherm models are presented in Figs. S-7 and  
 323 S-8. Looking at the data (TABLE II), on the basis of the  $R^2$  closest to 1 and the  
 324 lowest values of  $\chi^2$ , the following order of fitting equations is found to be:  
 325 Sips>Langmuir>Freundlich. The equilibrium parameters,  $R_L$ , calculated as  
 326  $R_L=1/(1+K_L C_0)$ , are falling in the range from 0.047 up to 0.889 in the investigated  
 327 concentration range. These values indicate that the removal of lead ions onto *A.*  
 328 *negundo* sorbents is favourable for all sorbents applied. The best fitting model  
 329 (Sips) of the sorption equilibrium is presented at Figure S-7. ANA has maximum  
 330 sorption capacity of 131.52 mg/g at 298 K while the lowest removal was achieved  
 331 by ANS application, 94.92 mg/g. Sips model implies that, in the same time,  
 332 monolayer sorption and heterogeneous energetic distribution of active sites on the  
 333 surface of the sorbent is possible.<sup>41</sup> Moreover, Sips model has been proven to be  
 334 applicable in cases of pH dependent sorption, such is the case of lead removal by  
 335 *A. negundo* sorbents.<sup>42</sup> TABLE III contains comparative data of investigated  
 336 materials sorption capacity with other similar lead sorbents found in the literature.  
 337 As can be seen, among three sorbent investigated in this study, the highest sorption  
 338 capacity is detected in ANA which is grown in uncontaminated habitat. This  
 339 indicates that the majority of the presented functional groups are available for  
 340 adsorption of  $Pb^{2+}$ . The lowest sorption capacity is detected in ANS, which  
 341 indicates lower availability of functional groups for  $Pb^{2+}$  adsorption due to their  
 342 current involvement in metal immobilization and/or different chemical  
 343 composition of leaves and different proportion of functional groups to which  $Pb^{2+}$   
 344 show high binding affinity.

345 TABLE II. Kinetic and isotherm parameters calculated for lead sorption by different sorbents

Kinetic models	ANA	ANV	ANS	Isotherm models	ANA	ANV	ANS
Experimental $q_e$ (mg/g)	86.62	83.81	73.25				
Pseudo-first-order				Langmuir			
$q_m$ (mg g <sup>-1</sup> )	84.76	83.10	71.86	$q_m$ (mg/g)	138.99	129.42	105.28
$k_f$ (min <sup>-1</sup> )	0.9584	1.410	0.6893	$K_L$ (dm <sup>3</sup> /mg)	0.0295	0.0360	0.0224
$R^2$	0.8320	0.7205	0.8035	$R^2$	0.995	0.991	0.988
$\chi^2$	3.5754	1.1044	8.4628	$\chi^2$	12.42	19.20	17.14
Pseudo-second-order				Freundlich			

$q_m$ (mg g <sup>-1</sup> )	86.04	83.66	73.67	$K_f$ (mg/g) (dm <sup>3</sup> /g) <sup>n</sup>	14.53	15.96	5.472
$k_2$ (g mg <sup>-1</sup> min <sup>-1</sup> )	0.0323	0.0830	0.0198	$1/n$	2.597	2.770	2.570
$R^2$	0.9744	0.9449	0.9706	$R^2$	0.920	0.904	0.895
$\chi^2$	0.5446	0.3380	1.2682	$\chi^2$	210.18	221.78	149.18
Elovich				Sips			
$q_m$ (mg g <sup>-1</sup> )	89.93	84.60	76.31	$q_m$ (mg/g)	131.52	120.18	94.92
$a$ (mg g <sup>-1</sup> min <sup>-1</sup> )	4.00E12	1.66E29	8.99E6	$K_s$ (dm <sup>3</sup> /g)	0.0205	0.0181	0.0090
$b$ (g mg <sup>-1</sup> )	0.3780	0.8548	0.2601	$s$	1.159	1.297	1.345
$R^2$	0.8108	0.8623	0.8531	$R^2$	0.997	0.998	0.985
$\chi^2$	4.0270	0.5442	6.3276	$\chi^2$	8.610	4.914	6.912

346 TABLE III. Comparison of lead sorption on various leaves sorbents

Sorbent / leaf powder	$q_m$ / mg/g	pH	$C_i$ / mg/dm <sup>3</sup>	Model
<i>Bael tree</i> <sup>43</sup>	4.065	5.0	25-100	Langmuir
<i>Cocos nucifera</i> <sup>44</sup>	8.475	5.0	10-150	Langmuir
<i>Ficus religiosa</i> <sup>45</sup>	37.45	4.0	10-1000	Langmuir
<i>Cinnamomum camphora</i> <sup>46</sup>	73.15	5.0	50-400	Langmuir
<i>B. papyrifera</i> <sup>47</sup>	84.74	5.5	10-500	Langmuir
<i>Aegle marmelos</i> <sup>48</sup>	104.0	5.1	8.7-180.2	Langmuir
<i>Citrus grandis</i> <sup>49</sup>	207.2	4.1	0-1000	Sips
<i>Acer negundo</i> (this study):				
ANA	131.5	5.0	5-600	Sips
ANV	120.2	5.0	5-600	Sips
ANS	94.92	5.0	5-600	Sips

347 Although this study showed that the sorption capacity of *A. negundo* leaf  
 348 powder in comparison to other sorbents with similar structure found in literature is  
 349 very high, it primarily emphasizes the importance of growing site on plant material  
 350 properties and its sorbent capacity. As found in this investigation, the variability  
 351 in sorption capacity may be significantly different among different samples and it  
 352 even reached 30%.

### 353 CONCLUSIONS

354 The presented investigation has shown that sorbents based on *A. negundo* L.  
 355 leaves are the promising sorbents for the removal of lead ions from contaminated  
 356 waters, but has also highlighted the importance of growing site as a factor affecting  
 357 the sorption performance of the future sorbent. Prior to the sorption experiments,  
 358 characterization of soils and leaves revealed differences between samples from  
 359 selected growing sites, particularly with respect to the content of PTE and CEC, as  
 360 well as differences in the presence of certain functional groups in *A. negundo*  
 361 leaves, responsible for sorption. The adsorption process was pH dependent and the  
 362 optimum pH for lead removal was 5.0, after 60 min of contact time, at optimized  
 363 sorbent dose of 2.0 g/dm<sup>3</sup>. The results of fitting experimental data showed that the  
 364 best fit was obtained by using the pseudo second order kinetic model, indicating  
 365 that the sorption mechanism is limited by binding forces through electrons sharing

366 between the lead ions and the sorbents. It was show that lead ions were removed  
 367 with a maximum lead loading capacity of the samples of 131.52 mg/g, 120.18 mg/g  
 368 and 94.92 mg/g for ANA, ANV, and ANS, respectively, which is either  
 369 comparable to or better than the lead loading capacities of other reported similar  
 370 sorbents. This research indicated that the differences in growing sites should be  
 371 taken into account when studying the sorption process, as they affect the adsorption  
 372 performance of the chosen biomass. Future studies could reveal the extent of this  
 373 influence on different sorbents and uncover the most influential site factors and  
 374 physiological mechanisms responsible for such outcome.

SUPPLEMENTARY MATERIAL

376 Additional data are available electronically at the pages of journal website:  
 377 <https://www.shd-pub.org.rs/index.php/JSCS/article/view/13367>, or from the corresponding  
 378 author on request.

379  
 380  
 381

382  
 383

384  
 385  
 386

387  
 388  
 389  
 390  
 391  
 392  
 393  
 394  
 395  
 396  
 397  
 398  
 399  
 400  
 401  
 402  
 403  
 404  
 405  
 406

407

408

## REFERENCES

- 409 1. D. Sikorska, P. Sikorski, P. Archiciński, J. Chormański, R. J. Hopkins, *Sustainability* **11**  
 410 (2019) 5838 (<https://doi.org/10.3390/su11205838>)
- 411 2. S. Dineva, *Dendrobiology* **53** (2005) 11-16 (<https://bibliotekanauki.pl/articles/41089.pdf>)
- 412 3. V. Stojanović, I. Bjedov, I. Jovanović, I. Jelić, D. Obratov Petković, M. Nešić, D.  
 413 Nedeljković, Odabrane invazivne strane vrste u flori Srbije – građa za izradu nacionalnog  
 414 propisa o sprečavanju unošenja i širenja invazivnih stranih vrsta i njihovom upravljanju.  
 415 Zavod za zaštitu prirode Srbije, 2021; Beograd
- 416 4. M. Akram, B. Khan, M. Imran, I. Ahmad, H. Ajaz, M. Tahir, F. Rabbani, I. Kaleem, M.  
 417 Akhtar, N. Ahmad, N. Samad Shah, *Int. J. Phytoremediat.* **21** (2019) 138  
 418 (<https://doi.org/10.1080/15226514.2018.1488810>)
- 419 5. I. Anastopoulos, A. Robalds, H. N. Tran, D. Mitrogiannis, D. A. Giannakoudakis, A.  
 420 Hosseini-Bandegharai, G. L. Dotto. *Environ. Chem. Lett.* **17** (2019) 755  
 421 (<https://doi.org/10.1007/s10311-018-00829-x>)
- 422 6. R. H. Krishna, W. B. Gilbert, *Int. J. Adv. Chem.* **2** (2014) 1  
 423 (<https://doi.org/10.14419/ijac.v2i1.1531>)
- 424 7. Official Gazette of RS, No. 102/2010: Decree on the Ecological Network
- 425 8. M. Glišić, D. Lakušić, J. Šinžar-Sekulić, S. Jovanović, *Bot. Ser.* **38** (2014) 131  
 426 ([https://botanicaserbica.bio.bg.ac.rs/arhiva/pdf/2014\\_38\\_1\\_604\\_full.pdf](https://botanicaserbica.bio.bg.ac.rs/arhiva/pdf/2014_38_1_604_full.pdf))
- 427 9. Official Gazette of RS, No. 102/2010: Decree on the Ecological Network
- 428 10. D. Filipović, Lj. Petrović, *Glas. Srp. geogr. druš.* **95** (2015) 109  
 429 (<https://doi.org/10.2298/GSGD1502109F>)
- 430 11. M. Kašanin-Grubin, S. Štrbac, S. Antonijević, S. Đogo Mračević, D. Randelović, I. Orlić,  
 431 A. Šajnović, *J. Environ. Manage.* **251** (2019) 109574  
 432 (<https://doi.org/10.1016/j.jenvman.2019.109574>)
- 433 12. S. Jarić, Z. Mataruga, D. Sekulić, M. Pavlović, D. Pavlović, M. Mitrović, P. Pavlović,  
 434 *Acta herbologica.* **29** (2020) 111-127 (<https://doi.org/10.5937/ActaHerb2002111J>)
- 435 13. D. Randelović, K. Jakovljević, T. Mišljenović, J. Savović, M. Kuzmanović, N.  
 436 Mihailović, S. Jovanović, *Water Air Soil Poll.* **231** (2020) 272  
 437 (<https://doi.org/10.1007/s11270-020-04655-2>)
- 438 14. ISO 11466 (1995) Soil quality-extraction of trace elements soluble in aqua regia. Geneva:  
 439 International Organization for Standardization.
- 440 15. JDPZ, Chemical methods for soil analysis, Beograd, 1966
- 441 16. J. Liang, H. L. Fang, T. L. Zhang, X. X. Wang, Y. D. Liu, *Urban For. Urban Green.* **27**  
 442 (2017) 390–398 (<https://doi.org/10.1016/j.ufug.2017.03.006>)
- 443 17. A. Sahay, A. Inam, A. Iqbal, *Int. J. Environ. Sci. Tech.* **17** (2019) 2889  
 444 (<https://doi.org/10.1007/s13762-019-02580-4>)
- 445 18. S. Stanković, T. Šoštarić, M. Bugarčić, A. Janićijević, K. Pantović-Spajić, Z. Lopičić,  
 446 *Acta Period. Technol.* **50** (2019) 268 (<https://doi.org/10.2298/APT1950268S>)
- 447 19. T. Šoštarić, M. Simić, Z. Lopičić, S. Zlatanović, F. Pastor, A. Antanasković, S.  
 448 Gorjanović, *Processes* **11** (2023) 1343 (<https://doi.org/10.3390/pr11051343>)
- 449 20. S. Sultan, *Trends Plant Sci.* **5** (2000) 537 ([https://doi.org/10.1016/S1360-1385\(00\)01797-0](https://doi.org/10.1016/S1360-1385(00)01797-0))
- 450 21. X. Ye, M. Wang, X. Zhang, R. Xu, D. Xu, *Env. Pollutants Bioavail.* **31** (2019) 240  
 451 (<https://doi.org/10.1080/26395940.2019.1630321>)
- 452 22. D. Stanković, M. Krstić, M. Knežević, M. Šijačić-Nikolić, I. Bjelanović, *Fresenius*  
 453 *Environ. Bull.* **21** (2012) 495
- 454 23. A. Kabata-Pendias, Trace elements in soils and plants. Boca Raton: CRC Press, Taylor &  
 455 Francis Group, 2011 (<https://doi.org/10.1201/b10158>)

- 456 24. X. Liu, D. S. Ellsworth, M. T. Tyree, *Tree Physiol.* **17** (1997) 169  
 457 (<https://doi.org/10.1093/treephys/17.3.169>)
- 458 25. M. Hasanuzzaman, M. H. M. B. Bhuyan, K. Nahar, M. S. Hossain, J. A. Mahmud, M. S.  
 459 Hossen, A. A. C. Masud, M. Moumita Fujita, *Agronomy* **8** (2018) 31  
 460 (<https://doi.org/10.3390/agronomy8030031>)
- 461 26. K. Drzewiecka, A. Piechalak, P. Goliński, M. Gąsecka, Z. Magdziak, M. Szostek, S.  
 462 Budzyńska, P. Niedzielski, M. Mleczek, *Chemosphere* **229** (2019) 589  
 463 (<https://doi.org/10.1016/j.chemosphere.2019.05.051>)
- 464 27. I. Van Dyck, N. Vanhoudt, J. Vives i Batlle, N. Horemans, A. Van Gompel, R. Nauts, J.  
 465 Wannijn, A. Wijgaerts, A. Vassilev, J. Vangronsveld, *Environ. Exp. Bot.* **213** (2023)  
 466 105440 (<https://doi.org/10.1016/j.envexpbot.2023.105440>)
- 467 28. R. Kashyap, R. Bajaj, S. Sajen, A. Raj, A. V. Jose, *Poll. Res.* **35** (2016) 403
- 468 29. R. Guderian, K. H. Becker, W. Fricke, R. Guderian, J. L. Löbeö, R. Rabe, U. Schurath,  
 469 D. T. Tingey, *Air Pollution by Photochemical Oxidants: Formation, Transport, Control,*  
 470 *and Effects on Plants*, Springer Science and Business Media, Springer Berlin Heidelberg,  
 471 ISBN 3642701183, 2012
- 472 30. T. Šoštarić, Z. Lopičić, D. Randelović, T. Rakić, A. Antanasković, I. Mikavica, J.  
 473 Milojković, in *Proceeding of 17<sup>th</sup> International Conference on Fundamental and Applied*  
 474 *Aspects of Physical Chemistry* (2024), Belgrade, Serbia, 459  
 475 (<https://doi.org/10.46793/Phys.Chem24II.459S>)
- 476 31. I. Mikavica, T. Šoštarić, A. Antanasković, D. Randelović, J. Petrović, G. Jovanović, Z.  
 477 Lopičić, in *Proceeding of VII International Congress "Engineering, Environment and*  
 478 *Materials in Process Industry"* (2021), Jahorina, 268
- 479 32. P. Y. Deng, W. Liu, B. Q. Zeng, Y. K. Qiu, L. S. Li, *Int. J. Environ. Sci. Tech.* **10** (2013)  
 480 559 (<https://doi.org/10.1007/s13762-013-0186-3>)
- 481 33. W. Azuma, S. Nakashima, E. Yamakita, H. R. Ishii, K. Kuroda, *Tree Physiol.* **37** (2017)  
 482 1367 (<https://doi.org/10.1093/treephys/tpx085>)
- 483 34. J. Ord, H. J. Butler, M. R. McAinsh, F. L. Martin, *Analyst* **141** (2016) 2896  
 484 (<https://doi.org/10.1039/C6AN00392C>)
- 485 35. K. Hasan, Y. Cheng, M. K. Kanwar, X. Y. Chu, G. J. Ahammed, Z. Y. Qi, *Front. Plant.*  
 486 *Sci.* **8** (2017) 1492 (<https://doi.org/10.3389/fpls.2017.01492>)
- 487 36. S. Qaiser, A. R. Saleemi, M. Umar, *J. Hazard. Mater.* **166** (2009) 998  
 488 (<https://doi.org/10.1016/j.jhazmat.2008.12.003>)
- 489 37. M. R. Sangi, A. Shahmoradi, J. Zolgharnein, G. H. Azimi, M. Ghorbandoost, *J. Hazard.*  
 490 *Mater.* **155** (2008) 513 (<https://doi.org/10.1016/j.jhazmat.2007.11.110>)
- 491 38. I. Langmuir, *J. Am. Chem. Soc.* **40** (1918) 1361 (<https://doi.org/10.1021/ja02242a004>)
- 492 39. H. M. F. Freundlich, *J. Phys. Chem.* **57** (1906) 385 (<https://doi.org/10.1515/zpch-1907-5723>)
- 493 40. R. Sips, *J. Chem. Phys.* **16** (1948) 490 (<https://doi.org/10.1063/1.1746922>)
- 494 41. S. Chowdhury, P. D. Saha, *Colloids Surf. B.* **88** (2011) 697  
 495 (<https://doi.org/10.1016/j.colsurfb.2011.08.003>)
- 496 42. V. J. Inglezakis, S. G. Pouloupoulos H. Kazemian, *Micropor. Mesopor. Mat.* **272** (2018)  
 497 166 (<https://doi.org/10.1016/j.micromeso.2018.06.026>)
- 498 43. P. S. Kumar, R. Gayathri, *J. Eng. Sci. Technol.* **4** (2009) 381  
 499 ([https://jestec.taylors.edu.my/Vol%204%20Issue%204%20December%2009/Vol\\_4\\_4\\_381\\_399\\_P.%20Senthil%20Kumar.pdf](https://jestec.taylors.edu.my/Vol%204%20Issue%204%20December%2009/Vol_4_4_381_399_P.%20Senthil%20Kumar.pdf))
- 500 44. H. Darla, P. Garimella, *Environ. Prog. Sustainable Energy* **38** (2019) S118  
 501 (<https://doi.org/10.1002/ep.12945>)
- 502  
 503

- 504 45. S. Qaiser, A. R. Saleemi, M. Umar, *J. Hazard. Mater.* **166** (2009) 998  
505 (<https://doi.org/10.1016/j.jhazmat.2008.12.003>)  
506 46. H. Chen, J. Zhao, G. Dai, J. Wu, H. Yan, *Desalination* **262** (2010) 174  
507 (<https://doi.org/10.1016/j.desal.2010.06.006>)  
508 47. U. M. K. Nagpal, A. V. Bankar, N. J. Pawar, B. P. Kapadnis, S. S. Zinjarde, *Water Air*  
509 *Soil Pollut.* **215** (2011). 177 (<https://doi.org/10.1007/s11270-010-0468-z>)  
510 48. S. Chakravarty, A. Mohanty, T. Nag Sudha, A. K. Upadhyay, J. Konar, J. K. Sircar, A.  
511 Madhukar, K. K. Gupta, *J. Hazard. Mater.* **173** (2010) 502  
512 (<https://doi.org/10.1016/j.jhazmat.2009.08.113>)  
513 49. L. B. L. Lim, N. Priyantha, Y. Lu, N. A. H. M. Zaidi, *Desalin. Water Treat.* **166** (2019)  
514 44 (<https://doi.org/10.5004/dwt.2019.24620>).



1 SUPPLEMENTARY MATERIAL TO  
2 **Comparative assessment of adsorbents performances of plant**  
3 **biomasses grown on different sites: case study of invasive**  
4 ***Acer negundo* L.**  
5 TATJANA ŠOŠTARIĆ<sup>1\*</sup>, ZORICA LOPIČIĆ<sup>1</sup>, DRAGANA RANĐELOVIĆ<sup>1</sup>, TAMARA  
6 RAKIĆ<sup>2</sup>, ANJA ANTANASKOVIĆ<sup>1</sup>, IVANA MIKAVICA<sup>1</sup> and SNEŽANA ZILDŽOVIĆ<sup>1</sup>  
7 <sup>1</sup>Institute for Technology of Nuclear and Other Mineral Raw Materials, Boulevard Franchet  
8 d'Esperey 86, 11000 Belgrade, Serbia, <sup>2</sup>University of Belgrade, Faculty of Biology, Studentski  
9 trg 16, 11000 Belgrade, Serbia  
10 J. Serb. Chem. Soc. 91 (0) (2026) 000–000

11 **Table S1.** Models used for evaluation of lead sorption onto investigated *A. negundo* sorbents

Model	Equation	Parameter
<i>Kinetic model</i>		
Pseudo-first order <sup>1</sup>	$\ln(q_e - q_t) = \ln q_e - k_1 t$	$q_e$ (mg/g): sorption capacity at equilibrium $q_t$ (mg/g): sorption capacity at any time $t$ $k_1$ (g/mg/min): the pseudo first order rate constant
Pseudo-second order <sup>2</sup>	$q_t = \frac{t}{\left(\frac{1}{k_2 q_e^2}\right) + \left(\frac{t}{q_e}\right)}$	$q_e$ (mg/g): sorption capacity at equilibrium $q_t$ (mg/g): sorption capacity at any time $t$ $k_2$ (g/mg/min): the pseudo second order rate constant
Elovich <sup>3</sup>	$q_t = \frac{1}{b} \ln(ab) + \frac{1}{b} \ln t$	$a$ (mg/g/min): initial Cu(II) sorption rate $b$ (g/mg): extent of surface coverage
<i>Isotherm model</i>		
Langmuir <sup>4</sup>	$q_e = \frac{q_m K_L C_e}{1 + K_L C_e}$	$q_m$ (mg/g): maximum sorption capacity $K_L$ (dm <sup>3</sup> /mg): Langmuir constant
Freundlich <sup>5</sup>	$q_e = K_f C_e^{1/n}$	$K_f$ (mg/g) (L/g) <sup>1/n</sup> : Freundlich constant $n$ : heterogeneity factor
Sips <sup>6</sup>	$q_e = \frac{q_m K_S C_e^s}{1 + C_e K_S^s}$	$K_s$ (dm <sup>3</sup> /g): Sips constant related to sorption affinity $s$ : heterogeneity factor

12  
13

\* Corresponding author. E-mail: t.sostaric@itnms.ac.rs

14 **TABLE S2.** Soil pH, SOC, oxido-reduction potential (Eh) and pseudo-total content of PTE,  
 15 and content of macroelements from the topsoil layer, together with mean values of PTE content  
 16 in leaves of ANA, ANV and ANS. Statistically significant differences are marked with asterisk  
 17 ( $p < 0.05 = *$ ,  $p < 0.01 = **$ ,  $P < 0.001 = ***$ )

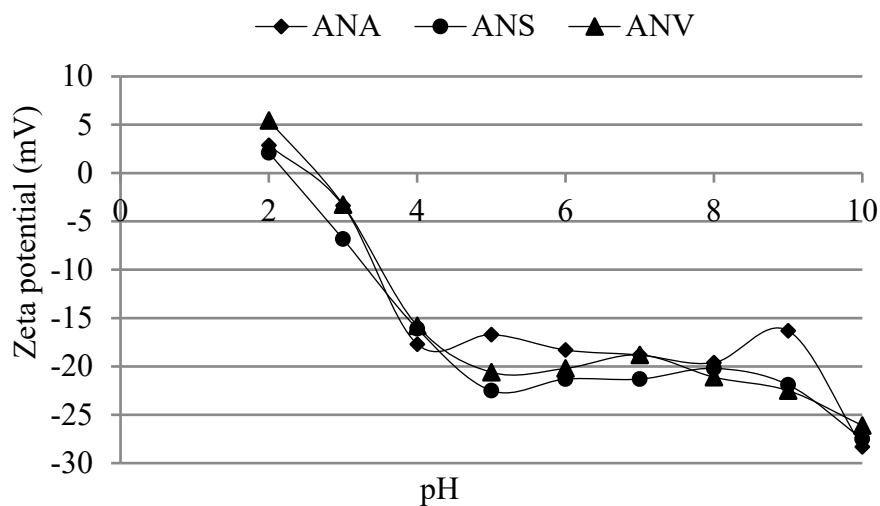
Ele. (ppm)	ANAs	ANVs <sub>s</sub>	ANS <sub>s</sub>		ANAL	ANVL	ANS <sub>L</sub>	
Cu	58.0 ± 0.1	31.9 ± 0.1	46.9 ± 1.0	***	19.9 ± 0.4	18.5 ± 0.5	15.7 ± 0.2	***
Fe	26,294 ± 182	28,994 ± 2044	41,817 ± 570	***	265 ± 32	222 ± 30	200 ± 13.7	
Ni	64.8 ± 5.0	63.2 ± 2.9	116 ± 6	***	34.9 ± 0.0	34.9 ± 0.2	44.9 ± 0.0	***
Mn	31.1 ± 0.1	34.2 ± 2.3	152 ± 7	***	45.9 ± 6.5	48.4 ± 0.0	12.2 ± 0.2	***
Cd	1.74 ± 0.24	1.5 ± 0.5	2.49 ± 0.00	**	n.d.	n.d.	1.24 ± 0.25	***
Pb	82.2 ± 2.2	39.9 ± 5.1	65.0 ± 4.8	***	n.d.	n.d.	n.d.	
Zn	234 ± 7	85.1 ± 6.9	95 ± 1	***	46.9 ± 1.4	48.8 ± 3.5	43.1 ± 2.7	
Ca	80,919 ± 991	11,354 ± 20	6,175 ± 59	***	51,413 ± 1,028	39,914 ± 473	26,430 ± 503	***
Na	226 ± 1	225 ± 16	406 ± 2	***	91.4 ± 18.3	88.8 ± 6	87.7 ± 19.9	
K	4,563 ± 132	5,514 ± 28	3,649 ± 4	***	14,334 ± 107	15,300 ± 276	17,417 ± 1,586	
Mg	16,308 ± 372	6,986 ± 487	6,038 ± 202		4,690 ± 540	4,415 ± 22	3,329 ± 38	***
pH	6.85 - 7.15	5.90 - 6.27	4.64 - 4.76					
Eh (mV)	271.0	212.2	370.2					
SOC (%)	4.0	3.4	2.6					

18 S – soil; L - leaf  
 19

20 **TABLE S3.** BCF<sub>L</sub> (soil to leaf) of PTE in ANA, ANV and ANS

Elements	ANA	ANV	ANS
Cu	0.34 ± 0.01	0.58 ± 0.01	0.34 ± 0.01
Fe	0.01 ± 0.001	0.01 ± 0.001	0.005 ± 0.0003
Ni	0.54 ± 0.04	0.55 ± 0.03	0.39 ± 0.02
Mn	1.48 ± 0.22	1.42 ± 0.09	0.08 ± 0.01
Cd	N/A	N/A	0.50 ± 0.10
Zn	0.20 ± 0.0004	0.58 ± 0.09	0.46 ± 0.03

21  
 22



23

24

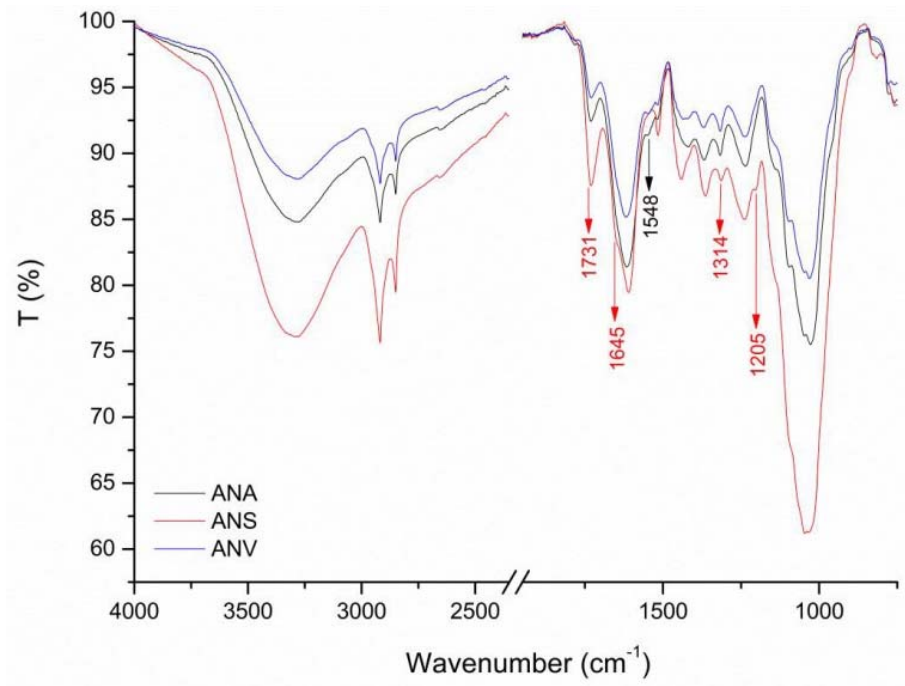
Fig. S-1. The zeta potential values of ANA, ANS and ANV under various pH values range

25

**TABLE S4.** Release of  $K^+$ ,  $Mg^{2+}$ ,  $Na^+$ ,  $Ca^{2+}$  and  $H^+$  due to biosorption of  $Pb^{2+}$

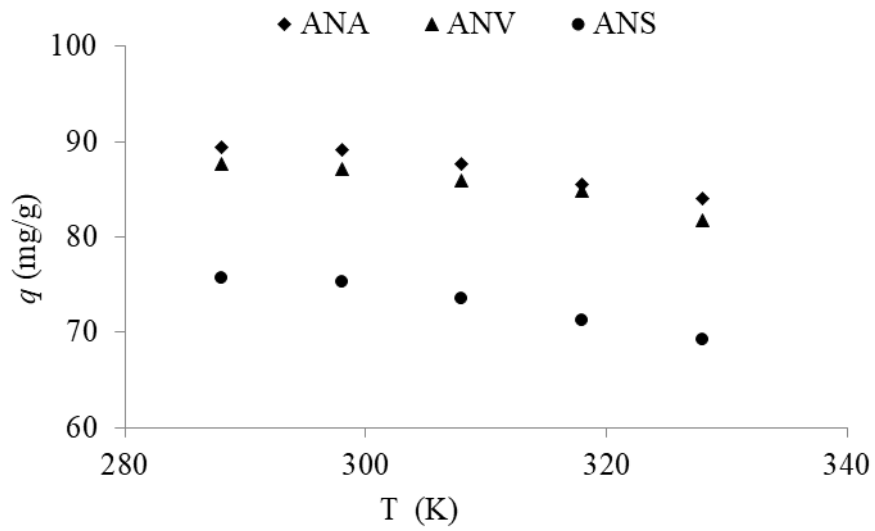
	Total metal bound						Net amount of cation released (meq/g)		
	$Pb^{2+}$	$K^+$	$Na^+$	$Mg^{2+}$	$Ca^{2+}$	$H^+$	$R_{b/r}$	pHi	pHf
ANA	43.45	5.0	0.4	12.2	23.0	5.0	0.95	5.0	3.91
ANV	45.56	8.2	0.3	8.9	18.7	6.3	1.07	5.0	3.86
ANS	45.07	15.5	0.25	9.8	33.7	8.0	0.67	5.0	3.77

26



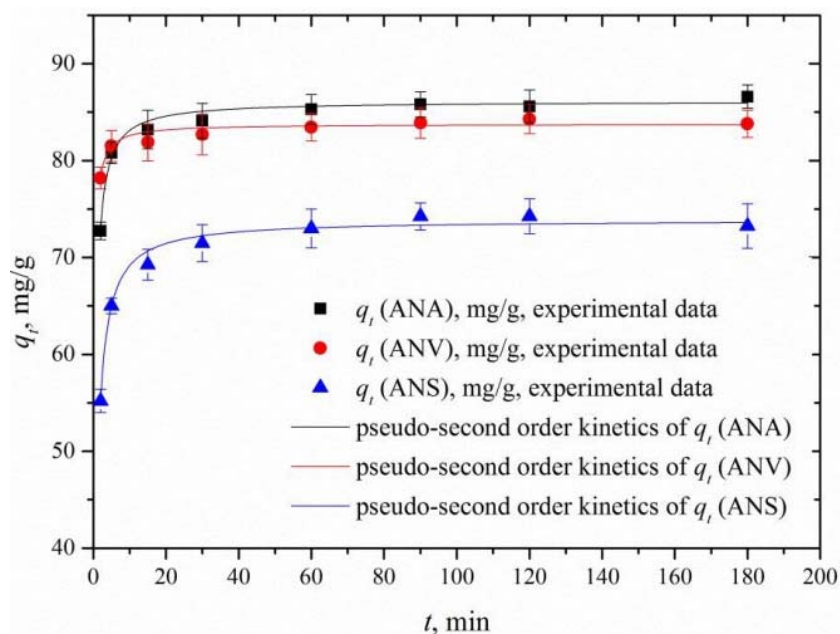
27  
28

Fig. S-2. ATR-FTIR spectra of all samples



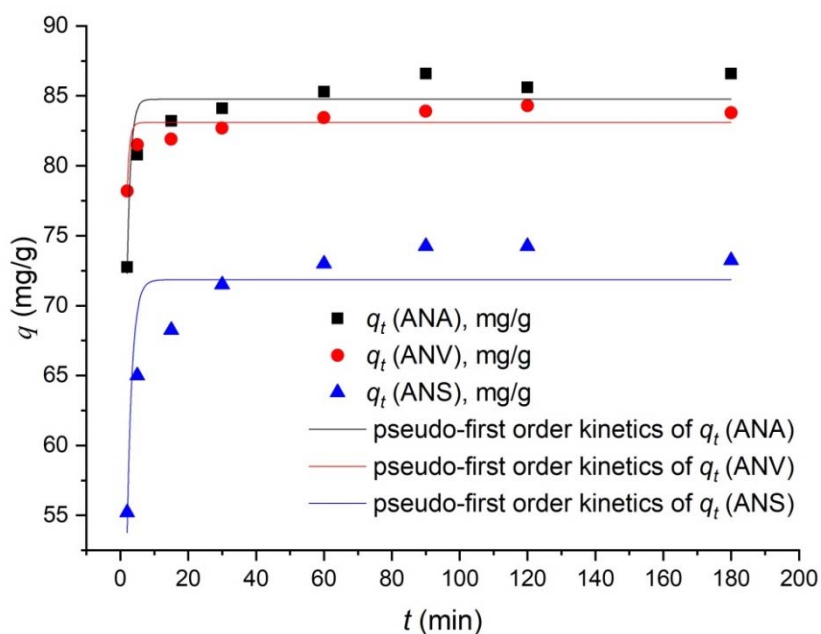
29  
30  
31

Fig. S-3. Effect of temperature on lead sorption capacity



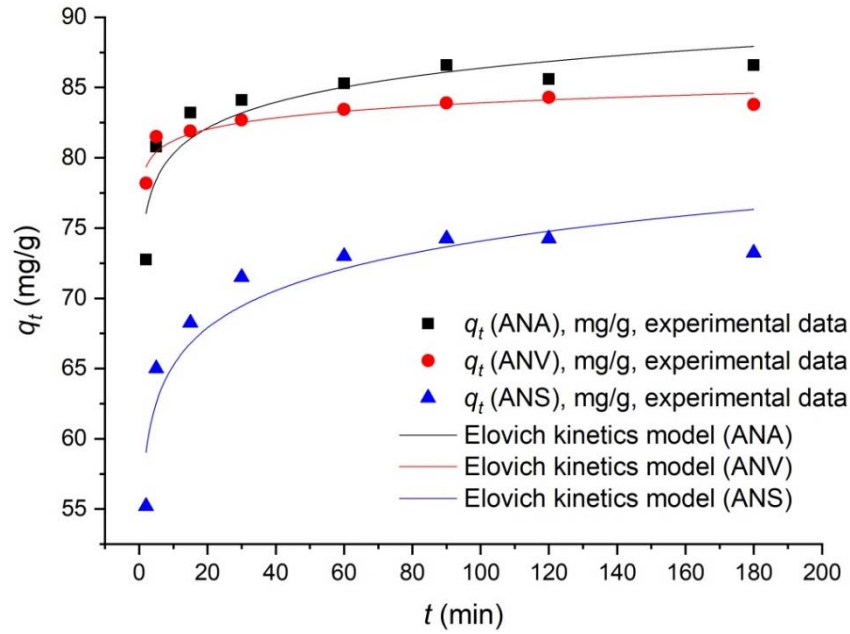
32  
33  
34  
35

Fig. S-4. Sorption kinetics: sorbed amount of lead per mass of sorbents ( $q_t$ ) as a function of time: experimental data (symbols) and the best fit predictions of the pseudo second order kinetics



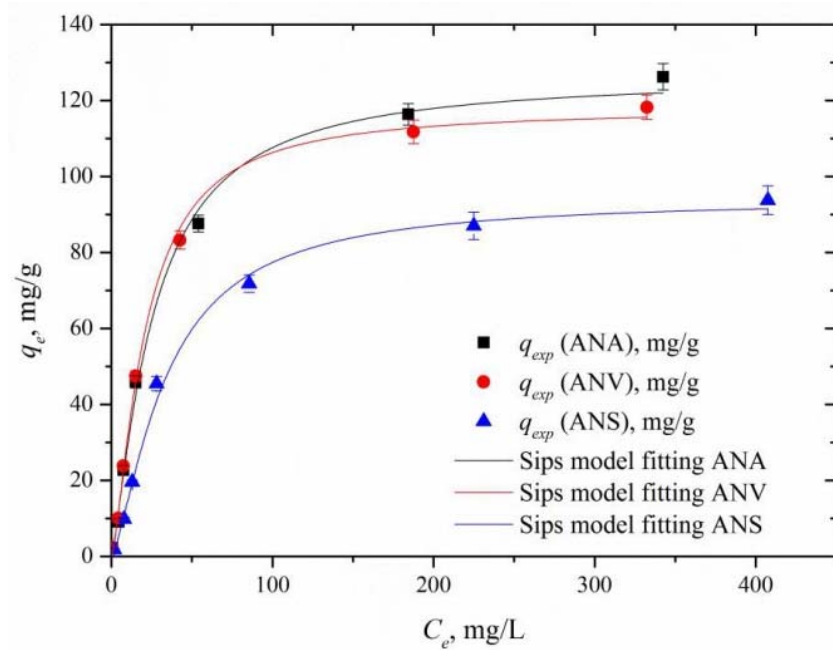
36  
37

Fig. S-5. Sorption kinetics: the pseudo first order kinetics



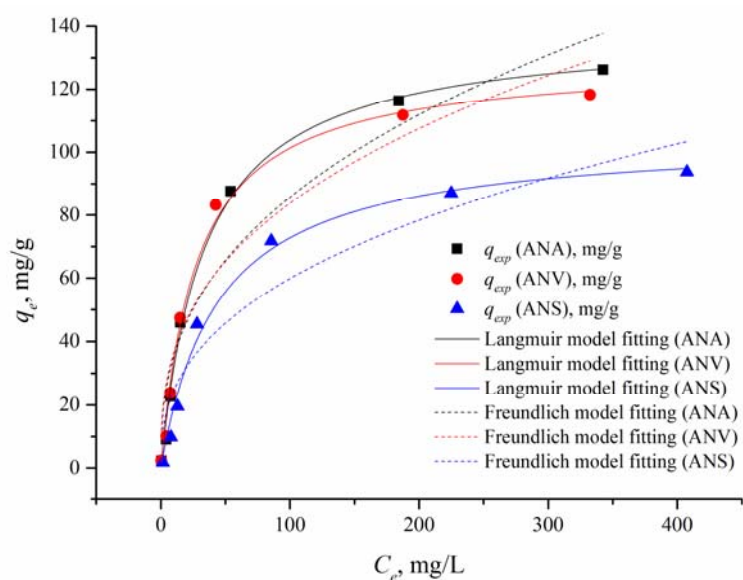
38  
39

Fig. S-6. Sorption kinetics: the Elovich model



40  
41  
42

Fig. S-7. Experimental isotherm data and nonlinear Sips model fit of lead sorption onto ANA, ANV and ANS



43

44

45

Fig. S-8. Experimental isotherm data and nonlinear Langmuir and Freundlich model fit of Pb(II) sorption onto ANA, ANV and ANS

46

47

## REFERENCES

48

1. S. Lagergren, *K. Sven. Veternskapsakad Handl.* **24** (1898) 1-39

49

2. Y. S. Ho, G. McKay, *Process Biochem.* **34** (1999) 451-465

50

([https://doi.org/10.1016/S0032-9592\(98\)00112-5](https://doi.org/10.1016/S0032-9592(98)00112-5))

51

3. M. J. D. Low, *Chem. Rev.* **60** (1960) 267-312 (<https://doi.org/10.1021/cr60205a003>)

52

4. I. Langmuir, *J. Am. Chem. Soc.* **40** (1918) 1361-1403

53

(<https://doi.org/10.1021/ja02242a004>)

54

5. H. M. F. Freundlich, *Zeitschrift für Physikalische Chemie* **57** (1907) 385-470

55

(<https://doi.org/10.1515/zpch-1907-5723>)

56

6. R. Sips, *J. Chem. Phys.* **16** (1948) 490-495 (<https://doi.org/10.1063/1.1746922>)

57